

B Δ P B Δ 424/1

## Size and depth of ancient magma reservoirs under atolls and islands of French Polynesia using gravity data

Valérie Clouard and Alain Bonneville

Laboratoire de Géosciences Marines et Télédétection, Université de la Polynésie Française  
Papeete, Tahiti, French Polynesia

Hans G. Barszczus,<sup>1</sup>

GBE - UMR 5569 - CNRS and Université de Montpellier II, Montpellier, France

**Abstract.** New insights into the structural and tectonic evolution of islands and atolls in French Polynesia are derived from the analysis of gravity data. Free-air anomaly maps were constructed using gravity data from land surveys of 25 islands combined with free-air anomaly data derived from satellite altimetry and shipborne gravimeters. Residual isostatic anomalies were calculated using a three-dimensional (3-D), four-layer crustal model taking into account the bathymetry of the seafloor, the topography of the islands, and the deflection of the lithosphere under the load of the volcanoes. Twenty of the 25 islands yield a positive residual anomaly, ranging between 9 and 60 mGal. Negative residual anomalies over four islands probably correspond either to limestone deposits or to fragmented material from aerial volcanism. The occurrence of a positive anomaly provides some evidence that there is a solidified magma chamber at depth beneath each of several islands in French Polynesia. A linear relation between the amplitude of the positive gravity anomaly and island volume is also observed. Geological features which generate these positive anomalies are described by simple geometric models (3-D ellipsoidal dense bodies) which lead to a rough estimate of the size and depth of the magma chambers. We then propose a simple linear relation between the volume of such magma chambers and the volume of islands that can be used for other extinct intraplate basaltic volcanoes. The diameter of the inferred magma chamber and its projection on the surface of the islands imply that calderas correspond mostly to collapses of the flanks of the edifices rather than to caldera vertical subsidence.

### 1. Introduction

French Polynesia (Figure 1) is located to the south of the central part of the Pacific Plate, between latitudes 5°S and 30°S and longitudes 130°W and 160°W. The Austral, Society, Pitcairn-Gambier, and Tuamotu island chains trend N120°, the same direction of the present Pacific Plate motion. The Marquesas Islands have a N140° strike. The region is crossed by the Austral and Marquesas Fracture Zones (FZ) with a N70° strike. These FZs are the main tectonic features of the seafloor and are related to the Farallon Ridge, which became extinct 9 Myr ago [Mammerickx *et al.*, 1980]. The average velocity of Pacific Plate motion is 11 cm

yr<sup>-1</sup> [Herron, 1972; Minster and Jordan, 1978]. The Austral, Society, Pitcairn-Gambier, and Marquesas island chains are composed mainly of islands, while the Tuamotu archipelago is composed entirely of atolls. All together, French Polynesia consists of 34 islands and 84 atolls.

The islands rise ~4500 m above the seafloor, and their maximum elevation above sea level, at Tahiti, is 2200 m. To a first approximation, island ages and morphologies are consistent with a hotspot theory: the age of each island within a chain increases from the southeast to the northwest, based on radiometric dating of volcanism from the present to about 16 Ma (Table 1). The age of the oceanic crust ranges between 45 and 85 Ma [Herron, 1972; Mayes *et al.*, 1990; Munsch *et al.*, 1996]. The Tuamotu Islands are separated from the other island chains by basins exceeding 5000 m in depth. The origin of the Tuamotu Islands, which rise above a broad plateau, is uncertain but has been attributed to an aborted ridge [Pautot, 1975], a hotspot [Okal and Cazenave,

<sup>1</sup>Also at Centre IRD, Montpellier, France

Copyright 2000 by the American Geophysical Union.

Paper number 1999JB900393.  
0148-0227/00/1999JB900393\$09.00

Fonds Documentaire IRD



010021578

8173

Fonds Documentaire IRD

Cote : B \* 21578 Ex : 7

ISSN



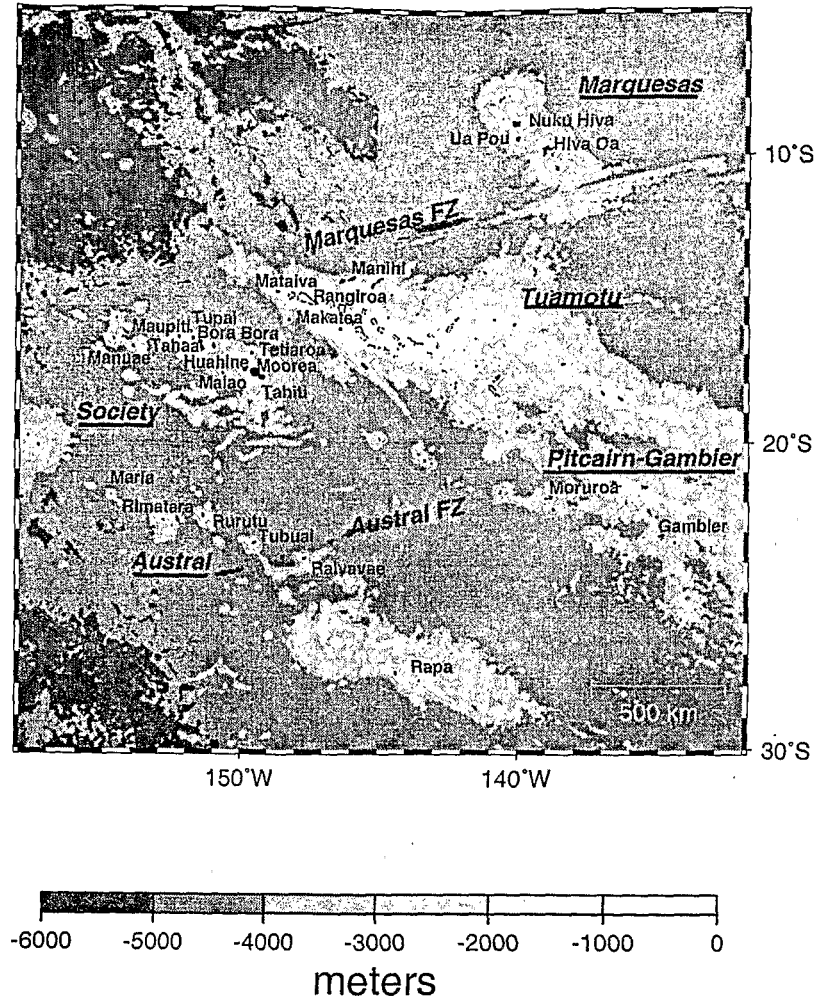


Figure 1. Bathymetric map [Sichoix and Bonneville, 1996] showing the volcanic chains of French Polynesia, with archipelago names underlined. The names of the islands discussed in text are shown. FZ stands for fracture zone.

1985], or an emerged submarine chain which originated close to the East Pacific Rise [Ito *et al.*, 1995].

The age, petrology, and geochemistry of the French Polynesian islands are relatively well known (see summaries by Brousse *et al.* [1990], Diraison [1991], and Leroy [1994]), but their subsurface structure, apart from Moruroa and Fangataufa atolls [Guille *et al.*, 1992, 1993], remains poorly known. In this paper, we address the lateral density distribution using existing gravity data, which leads to a three-dimensional model of the islands. Shipboard and satellite-derived gravity data are merged with previously unpublished land data. After adjusting these different data sets to a common reference system, a free-air anomaly (FAA) map is obtained. We then subtract a theoretical gravity field computed using a three-dimensional, four-layer crustal model based on a digital terrain model (for bathymetry and elevation). Residual isostatic anomaly maps [Blakely, 1995] are then produced for 17 islands and 8 atolls to obtain insights into the makeup of shield volcanoes.

## 2. Data Presentation and Processing

### 2.1. Gravity Data

From 1978 to 1981, 800 measurements were made by Barszczus [1979, 1980, 1981] using a Worden 600 gravimeter at Manuae, Maupiti, Tupai, Bora-Bora, Tahaa, Huahine, Maiao, Tetiaroa, Moorea, and Tahiti in the Society Islands; Nuku Hiva, Hiva Oa, and Ua Pou in the Marquesas Islands; Maria, Rimatara, Rurutu, Tubuai, Raiavavae, and Rapa in the Austral Islands; Moruroa and Gambier Islands in Gambier-Pitcairn alignment; and Mataiva, Manihi, Makatea, and Rangiroa in the Tuamotu Islands. These data were merged with 137 measurements made by Macheski [1965] at Tahiti and Moorea using a Worden 300 gravimeter and with 320 measurements made by Leroy [1994] at Tahiti using a Lacoste and Romberg model G gravimeter. All data are tied to PPT J7912, a reference station of the International Gravity Standardization Net established in 1971 (IGSN71) and located at Pamatai in Tahiti. The PPT J7912 station (where PPT stands for Papeete and J7912

Table 1. Radiometric Ages of Aerial Volcanism in French Polynesian Studied Islands

Island	Longitude W	Latitude S	Age, Ma	Reference
Austral				
Raivavae	147°39'	23°52'	5.6-7.6	<i>Duncan and McDougall</i> [1976]
Rapa	144°20'	27°36'	5.9-5.2	<i>Krummenacher and Noetzlin</i> [1966]
Rimatara	152°48'	22°39'	(4.8-28.6)	<i>Turner and Jarrard</i> [1982]
Rurutu	151°21'	22°29'	0.6-12.3	<i>Dalrymple et al.</i> [1975], <i>Duncan and McDougall</i> [1976], and <i>Turner and Jarrard</i> [1982]
Tubuai	149°30'	23°23'	8.5-10.6	<i>Duncan and McDougall</i> [1976]
Marquesas				
Hiva Oa	139°03'	09°45'	1.6-2.5	<i>Duncan and McDougall</i> [1974]
Nuku Hiva	140°12'	08°54'	3.0-4.3	<i>Duncan and McDougall</i> [1974]
Society				
Bora Bora	151°44'	16°30'	3.1-3.4	<i>Duncan and McDougall</i> [1976]
Huahine	151°00'	16°45'	2.0-2.6	<i>Duncan and McDougall</i> [1976]
Maupiti	152°16'	16°27'	4.0-4.5	<i>Duncan and McDougall</i> [1976]
Moorea	149°50'	17°33'	1.5-1.7	<i>Duncan and McDougall</i> [1976]
Tahaa	151°30'	16°39'	2.6-3.2	<i>Duncan and McDougall</i> [1976]
Tahiti-iti	149°30'	17°36'	0.4-0.5	<i>Leroy</i> [1994]
Tahiti-nui	149°15'	17°48'	0.19-1.37	<i>Leroy</i> [1994]
Pitcairn-Gambier				
Gambier (Manureva)	134°57'	23°09'	6.2	<i>Guillou et al.</i> [1994]
Moruroa	138°54'	21°51'	11.0	<i>Gillot et al.</i> [1992]

means that it was the twelfth station made in 1979) was established by a Japanese team during a circum-Pacific gravimetric connections campaign [Nakagawa et al., 1983]. From this total "land data set", a FAA was then calculated using the GRS80 ellipsoid model. The experimental error  $e$  related to this land data set can be expressed as the sum of the measurement error  $e_m$  estimated to be 0.35 mGal (standard deviation [Barszczus, 1980]) and a function of the barometric leveling error  $dz$  estimated to be 10 m, as follows:

$$e = e_m + 0.3086 dz \cong 3.5 \text{ mGal.} \quad (1)$$

Marine gravity data for the area compiled by *Sichoix and Bonneville* [1996] include 27 tracks (116,171 points) from the National Geophysical Data Center (NGDC) database which was obtained with good satellite navigation accuracy. After the removal of uncontrolled peaks, this set was tied to a Seasat and ERS-1 satellite-derived FAA grid [Smith and Sandwell, 1995]. We have added data from recent cruises in French Polynesia to the *Sichoix and Bonneville* [1996] data set: EW9602 on the R/V Maurice Ewing to the southeast of the Austral Islands [McNutt et al., 1997] and two cruises on the R/V L'Atalante, ZEPOLYF1, south of the Society Islands [Bonneville et al., 1997] and ZEPOLYF2, north

of the Austral Islands (*A. Bonneville, personal communication*, 1999). The entire offshore data set is referred to here as the "marine data set." The error on FAA satellite-derived data was estimated to be 5 mGal by *Sandwell* [1992]. The shipboard data error is 1 to 2 mGal. Consequently, a maximum error of 5 mGal for the whole marine data set is assumed.

## 2.2. Free-air Anomaly Maps

When preparing composite FAA maps, the first adjustment of land and marine gravity data is controlled visually. Close to lands, the values in the marine data set, composed mainly of satellite data, appear systematically lower by a few tens of milliGals than the ground data set. This discrepancy may be related to (1) the hanging of radar beams on island flanks [Barriot, 1987]; (2) a bias introduced from the method to produce gravity fields from the geoid signal due to crossover of unevenly spaced ground tracks, especially in the vicinity of islands where data have been removed [Filmer, 1991]; and (3) the size of the island itself when its diameter ranges from 5 to 15 km, which is close to the resolution of the satellite (20-30 km, [Sandwell, 1992]).

To adjust these two data sets, we used only shipboard data in the vicinity of islands (up to 6 km offshore, ex-

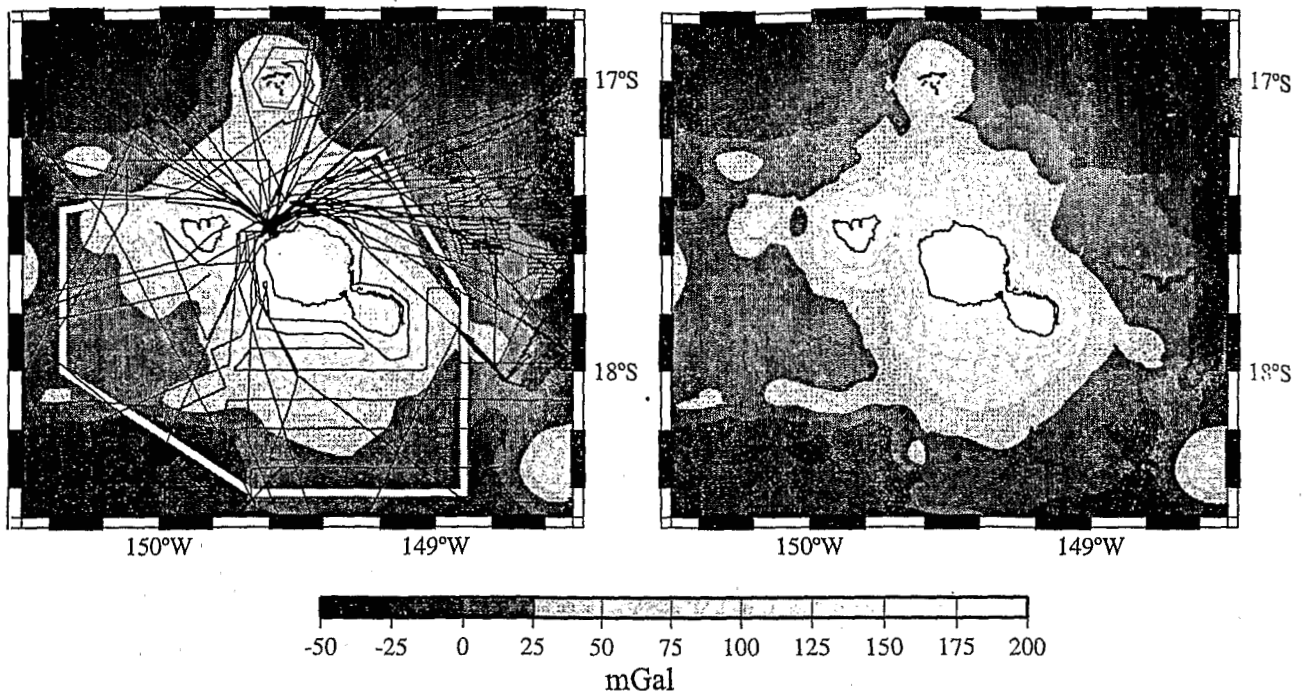


**Figure 2.** Example of the derivation of the FAA map for the Tetiaroa, Moorea, and Tahiti islands. (left) Gravity satellite data only [Smith and Sandwell, 1995]. The thin black lines represent the shipboard profiles along which the measured gravity values were used to produce an improved field within the polygons shown as white lines. (right) Final FAA map produced by merging the satellite data outside the polygons with the shipborne data within the polygons. Note the improvement in anomaly resolution over and near the islands. Contour interval is 25 mGal.

cept for Tahiti where this limit is extended to 60 km) because these data have the same reference bases as the ground data and thus their datum are comparable (Figure 2). Using a continuous curvature "splines-in-tension" algorithm (GMT [Smith and Wessel, 1990]), the land data set and shipboard data in the vicinity of islands were merged with the complete marine data set minus the data around the islands to obtain two types of grids. The first grid corresponds to the complete FAA map of French Polynesia, which is a coarse grid 2'x2', such as is shown in the small region around the island of Tahiti in Figure 2. The second type corresponds to a set of finer grids covering each island, which were used in calculating the properties and geometry of magma chambers. These are 30''x30'' grids, constrained by good spatial coverage on land (1352 measurements for 2350km<sup>2</sup>, averaging about two stations within a 60''x60'' area). (All the grids are available at URL <http://www.ipgp.jussieu.fr/UFP/download.html>.)

### 2.3. Topographic Maps

We used the synthesized database of bathymetry compiled by Sichoix and Bonneville [1996] that was based on ~82 cruises plus additional soundings from the French Service Hydrographique et Océanographique de la Marine, all acquired with satellite navigation since

1967. Data were carefully checked for quality and subjected to a crossover analysis, similar to the one used by Smith [1993], but using Global Positioning System (GPS) navigated expeditions for reference. The most recent bathymetric profiles used, including multi-beam soundings from EW9602 and ZEPOLYF1 cruises, are denser, often with a spacing of <500 m along the shiptrack. The older profiles have a typical spacing of >2 km.

Elevation data on islands were obtained by digitizing topographic maps of French Polynesia [Service de l'Urbanisme, 1992] and from maps of the Atlas de la Polynésie Française [ORSTOM, 1993]. For the island of Tahiti we used a digital terrain model derived by Géoimage (Sophia Antipolis, France) from two stereoscopic SPOT images. The elevation on atolls was arbitrarily set at 0 m over the lagoon (for depths between 1 and 40 m) and at 1 m above sea level on the coral rim (for heights between 1 and 5 m). Topographic land data and bathymetric data were then combined and gridded to produce a 2'x2' grid for the whole area, and several 30''x30'' grids covering each island.

### 2.4. Flexural Model

Previous studies of the gravity and topography of the Hawaiian archipelago [e.g., Walcott, 1970] show that

volcanic loads on the oceanic lithosphere are supported regionally rather than locally. In response to applied loads the lithosphere acts as a thin elastic plate overlying an inviscid fluid [Watts *et al.*, 1980]. The amplitude of the deflexion depends on both the size of the volcanic load and the effective flexural rigidity of the thin elastic plate [Watts *et al.*, 1975]. The flexural rigidity is linked to the elastic thickness of the lithosphere that corresponds to the upper part of the lithosphere and depends mainly on the temperature, and hence on the age of the lithosphere at the time of loading [Watts, 1978].

Watts and Ribe [1984] obtained several values of the flexural rigidity in various tectonic contexts. McNutt [1984] introduced the concept of the "effective thermal age," which corresponds to the thermal age at the time of loading. It can be less than the lithospheric age if the plate has been reheated, which is common for regions

of intraplate volcanism. Calmant and Cazenave [1986] and Young and Hill [1986] invoke this concept to explain rigidity anomalies obtained below the Cook, Austral, and Society Islands and below the Cape Verde rise.

The numerical and three-dimensional approach developed by Watts *et al.*, [1975] is used here to solve the classical equation governing the deformation  $w$  (positive downward) of an elastic layer under a volcanic load:

$$D\nabla^4 w + (\rho_m - \rho_l)gw = q(x, y) \quad (2)$$

where  $\rho_l$  is the load density,  $\rho_m$  is the mantle density,  $D$  the flexural rigidity of the lithosphere,  $\nabla$  is the bi-harmonic operator,  $q(x, y)$  is the vertical load derived from the topographic grid obtained previously, and  $g$  is the acceleration due to gravity ( $g = 9.81 \text{ m s}^{-2}$ ).

In our study the value of  $D$  has been carefully chosen for each island group using two methods. In the first

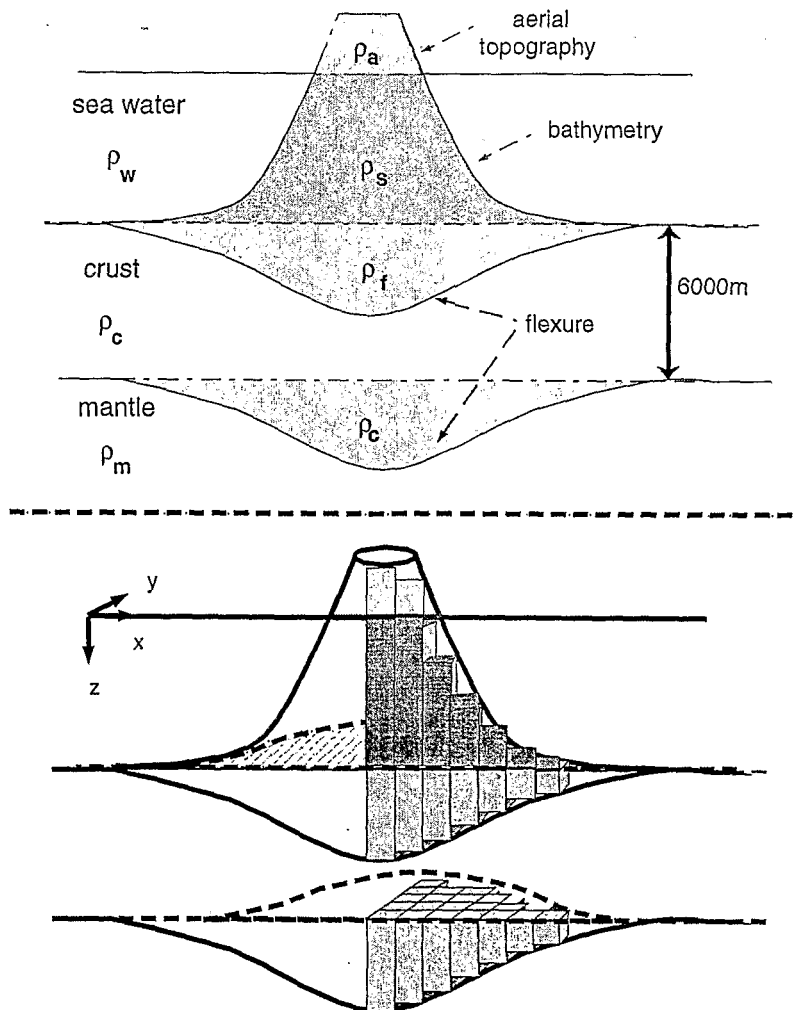


**Figure 3.** The theoretical FAA is obtained by computing the gravity effect of volcanic construction above a deflected crust. (top) The model involves six layers, with different densities  $\rho$ . The assumed densities for crust ( $\rho_c$ ), mantle ( $\rho_m$ ), and water ( $\rho_w$ ) are  $2900$ ,  $3350$  and  $1030 \text{ kg m}^{-3}$ , respectively. The deflection is estimated using a 3-D model for a thin elastic plate loaded by the topography (see text). The volcanic load is modeled by three layers: the subaerial volcanic construction ( $\rho_a$ ), the submarine volcanic construction ( $\rho_s$ ), the material filling the flexure ( $\rho_f$ ) with  $\rho_a < \rho_s < \rho_f$ . (bottom) The geometry of the system is modeled by elementary prisms.



method, seismic refraction profiles provide the Moho depth (Society and west Tuamotu Islands [Danobeatia *et al.*, 1995; Talandier and Okal, 1987] and Marquesas Islands [Caress *et al.*, 1995]). After this depth is compared with the Moho depth based on the flexural model we select the  $D$  value that minimizes the difference between observations and model. In the second method, employed when seismic refraction data are unavailable, we used published  $D$  values. Typical values of  $D$  vary from  $1.5 \times 10^{21}$  N m to  $8.0 \times 10^{22}$  N m for the south central Pacific area [e.g. Calmant and Cazenave, 1987; Filmer *et al.*, 1993; Goodwillie and Watts, 1993]. These are much lower than the values expected for the range of crustal ages concerned [Watts *et al.*, 1980]. Complete discussions of the choice of flexural rigidity values for our region are given by McNutt [1998] and Sichoix [1997]. The following values for the flexural rigidity were selected:  $4.0 \times 10^{22}$  N m for Society and Marquesas Islands,  $3.5 \times 10^{21}$  N m for Pitcairn-Gambier Islands,  $1.2 \times 10^{22}$  N m for western Austral Islands,  $3.5 \times 10^{21}$  N m for the eastern Austral Islands, and  $8.0 \times 10^{21}$  N m for Tuamotu Islands. We assume that the representative densities of the mantle and the load are  $\rho_m = 3350$  kg m $^{-3}$  and  $\rho_l = 2700$  kg m $^{-3}$  respectively [Caress *et al.*, 1995; Sichoix, 1997]. The deflection  $w$  is then computed for all the nodes ( $2' \times 2'$ ) of the topographic grid.

### 2.5. Isostatic Residual Anomaly

A three-dimensional, four-layer crustal model (Figure 3) is used to compute a theoretical FAA. The interface between the ocean and seafloor is given by the bathymetric grid (Figure 1). The interface between the volcanic load, divided into three density layers, and the oceanic crust is given by the deflection grid, which is assumed also to define the interface between crust and mantle. The crust is assumed to have a constant thickness of 6000 m. This thickness has been determined from seismic refraction studies in the Society-Tuamotu area [Danobeatia *et al.*, 1995] and the Marquesas area [Caress *et al.*, 1995]. The material filling the depressions under the load is assumed to have a higher density ( $\rho_f$ ) than the overlying volcanic material ( $\rho_s$ ) and the aerial part of the volcano ( $\rho_a$ ). The seafloor normal depth is given by the deepest point of the bathymetric grid within the particular area being studied. The model is divided into  $2' \times 2'$  square prisms extending to Moho depth. The zero FAA is given by a flat oceanic crust at the sea floor normal depth. The theoretical FAA is then computed for each node of the  $2' \times 2'$  grid by summing the gravity effects of all the prisms [Plouff, 1976] produced by the density contrasts shown in Figure 3. A similar computation was made for each island using the finer grid ( $30'' \times 30''$ ).

By subtracting the theoretical FAA grid from the observed anomaly, an isostatic residual gravity field [Blakely, 1995], similar to an isostatic Bouguer field (Figure 4), is determined and investigated below as to

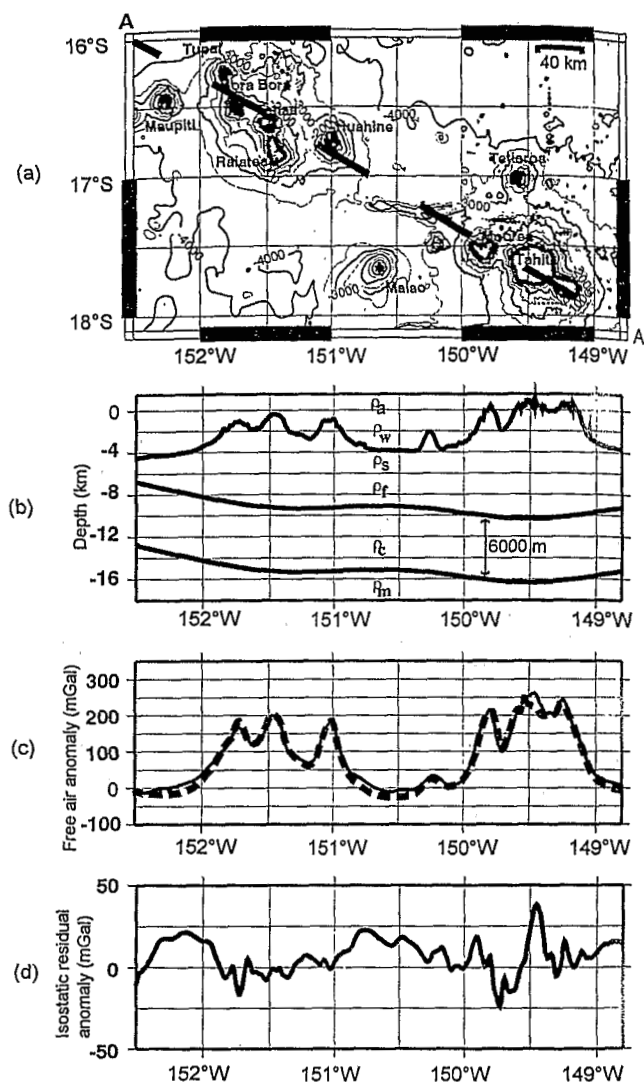


**Figure 4.** Residual isostatic anomaly over the Society Islands obtained by subtracting the modeled FAA from the observed. (a) Bathymetric map of the Society Islands. Data along the profile AA' (solid dashed line) are shown in Figures 4b, 4c and 4d; (b) the crustal model used to compute the modeled FAA. The elastic thickness is adjusted using the Moho depth given by seismic refraction profiles; (c) comparison between observed (thick dashes) and computed FAA (thin line) along AA'; and (d) isostatic residual gravity anomaly along AA'.

its utility to provide new insights on the makeup of islands. According to Figure 3, only contrasts between mantle and crustal densities and between crust and infill densities are relevant in the model, not their absolute values. As the density contrasts are regional parameters rather than specific to each island, we determined these contrasts by minimizing the difference between computed and observed gravity anomaly for each archipelago. The best estimate of the mantle-crust density contrast is everywhere  $450$  kg m $^{-3}$ . Assuming a value of  $3350$  kg m $^{-3}$  for the mantle density, the crust density is then  $2900$  kg m $^{-3}$ . Thus the volcano submar-

Table 2. Properties of Islands Showing Positive Residual Isostatic Anomalies

Island	Island Volume, $V_v$ , km <sup>3</sup>	Caldera Diameter, km	Filling Density $\rho_f$ , kg m <sup>-3</sup>	Submarine Density $\rho_s$ , kg m <sup>-3</sup>	Amplitude $g_{max}$ , mGal	Half Wavelength* km	Location
Austral							
Raiavavae	2159	3	2900	2900	16	7	south island centered
Rapa	1500	3.5 and 5	2850	2500	17	7	caldera centered
Rurutu	1950	none	2900	2900	16	7.5	island centered
Tubuai	3273	2	2850	2750	26	11	west caldera centered
Marquesas							
Hiva Oa	7628	10 and 15	2800	2700	35	18	caldera centered
Nuku Hiva	5811	6 and 9	2800	2800	29	19	east caldera centered
Ua Pou	2771	none	2800	2650	10	?	not enough points
Society							
Bora Bora	2338	3	2900	2900	16	6	caldera centered
Huahine	2636	drowned	2850	2850	17	7	island centered
Maiao	1857	3	2850	2700	11	3	caldera centered
Manuae	2302	atoll	2800	2550	17	7	east lagoon centered
Maupiti	2132	drowned	2900	2850	18	5	caldera centered
Moorea	3166	9	2850	2700	30	10	island centered
Tahaa	2784	4	2900	2700	21	12	caldera centered
Tahiti	12914	8	2900	2650	60	24	caldera centered
Tetiaroa	1300	atoll	2850	2650	11	4	lagoon centered
Tupai	1442	atoll	2850	2800	111	5	lagoon centered
Tuamotu-Gambier							
Gambier	7287	drowned	2800	2600	34	15	caldera centered
Moruroa	4497	atoll	2600	2300	22	14	south lagoon centered
Rangiroa	14668	atoll	2750	2550	23	30	lagoon centered

\*The half wavelength represents the anomaly width.

ine density  $\rho_s$ , and, to a lesser extent, the infill density  $\rho_f$  are the main factors controlling our models. These parameters are varied in the range 2300 to 2900 kg m<sup>-3</sup> and the residual anomaly is minimized by the technique of least squares.

With this approach, we determined characteristic submarine and filling densities for each of the 25 islands considered (Table 2). The average values of  $\rho_s$  and  $\rho_f$  for all islands are 2700 and 2800 kg m<sup>-3</sup>, respectively (discussed later).

### 3. Results and Analysis

Twenty of the 25 islands yield a gravity residual anomaly >5 mGal, the assumed uncertainty. The residual anomalies for these 20 islands are shown in Figures 5 to 8. To a first approximation, the contours are concentric, and their amplitude ranges from -20 to +60 mGal. Their wavelengths are similar to the diameter of the volcanoes, suggesting that the anomalies are related to density contrasts at depth within the volca-

noes. *Machesky* [1965] related positive Bouguer anomalies to gabbros which outcrop in the caldera of Tahiti. More generally, *Rymer and Brown* [1986] proposed a classification of gravity anomalies in which positive anomalies characterize mainly basaltic volcanoes and are caused by a relatively dense intrusive complex/magma body which contrasts with its surroundings. Because the French Polynesian islands are basaltic shield volcanoes, a pronounced positive anomaly mostly expresses the dense cumulate core or solidified magma chamber of the volcano. We will use known geological settings to refine the relation between a positive gravity anomaly and a dense intrusive complex, in order to establish a typology of gravity fields over the Polynesian volcanoes. Our results are sorted by archipelago and are shown in Table 2 and Table 3 according to the sign (+/-) of the residual anomaly.

#### 3.1. Society Islands

The age of the oceanic crust in the chain of the Society Islands ranges from 65 Ma in the south to 80 Ma



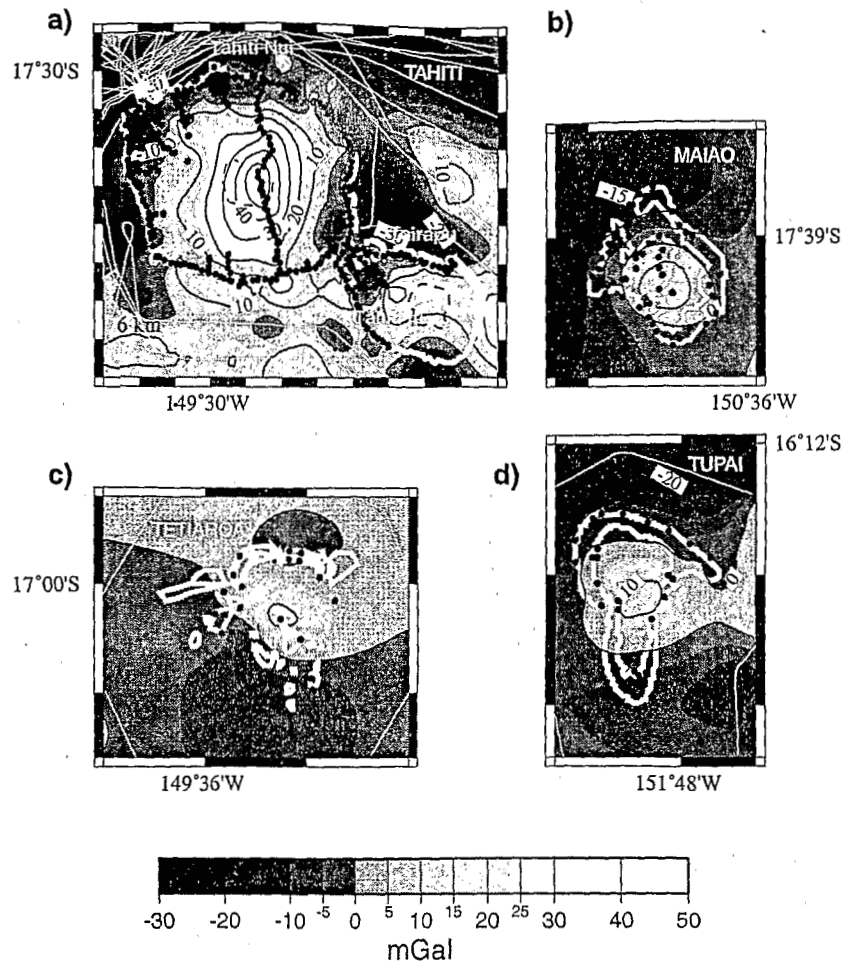


**Figure 5.** Isostatic residual anomaly over individual islands of the Society Island chain where a residual anomaly greater than 5 mGal is observed. (a) Tahiti, (b) Maiao, (c) Tetiaroa, (d) Tupai, (e) Manuae, (f) Huahine, (g) Tahaa, (h) Moorea, (i) Bora Bora, (j) Maupiti. Black dots represent land gravity stations, and black dashed lines represent caldera boundaries. Thick white lines represent the coast, and thin white lines represent the marine gravity data.

750 km away in the north [Herron, 1972; Mayes et al., 1990]. This island chain is composed of five atolls and nine islands of which Maupiti is the oldest (about 4.3 Ma [Duncan and McDougall, 1976]) and Mehetia the youngest (0 to 0.3 Ma [White and Duncan, 1996]). Because Mehetia is associated with the present hotspot, it has been intensely studied over the past 15 years [Talandier and Okal, 1984a; Cheminée et al., 1990; Binard et al., 1991]. The geochronology, geochemistry, volcanology, and geology of the Society Islands have been reviewed in some detail by Diraison et al. [1991] and more recently by White and Duncan [1996]. The aerial activity of these volcanoes can be described by three main sequential stages: the edification of a shield volcano, the formation of a caldera, and the occurrence of postcaldera volcanism.

Figure 5 shows the residual gravity anomaly over 10 islands of the Society group. Owing to the relatively dense coverage of bathymetry and gravity data, results for these islands are probably more reliable than those

for the other islands studied here. Positive anomalies are present at all of the islands and atolls (Figure 5) and range from 60 mGal over Tahiti (Figure 5a), the largest island, to 11 mGal over Maiao (Figure 5b), the smallest island, and Tetiaroa (Figure 5c), the smallest atoll (Table 2). In the case of the islands the positive anomalies are located over the inferred centers of the main feeding systems and have wavelengths similar to the diameter of the islands or the calderas. Positive anomalies are usually related to shield volcanoes and reflect a deep-seated, solidified magma chamber or feeding system [Rymer and Brown, 1986]. Thus the positive anomalies over the atolls of Tetiaroa (Figure 5c), Tupai (Figure 5d), and Manuae (Figure 5e) may express underlying dense magma chambers.

Tahiti is composed of two different volcanoes, Tahiti Nui and Tahiti Iti on the peninsula. There are sufficient gravity data on Tahiti Nui to establish the existence of a correlation between the positive anomaly and the caldera. On the other hand, the data coverage for Tahiti Iti

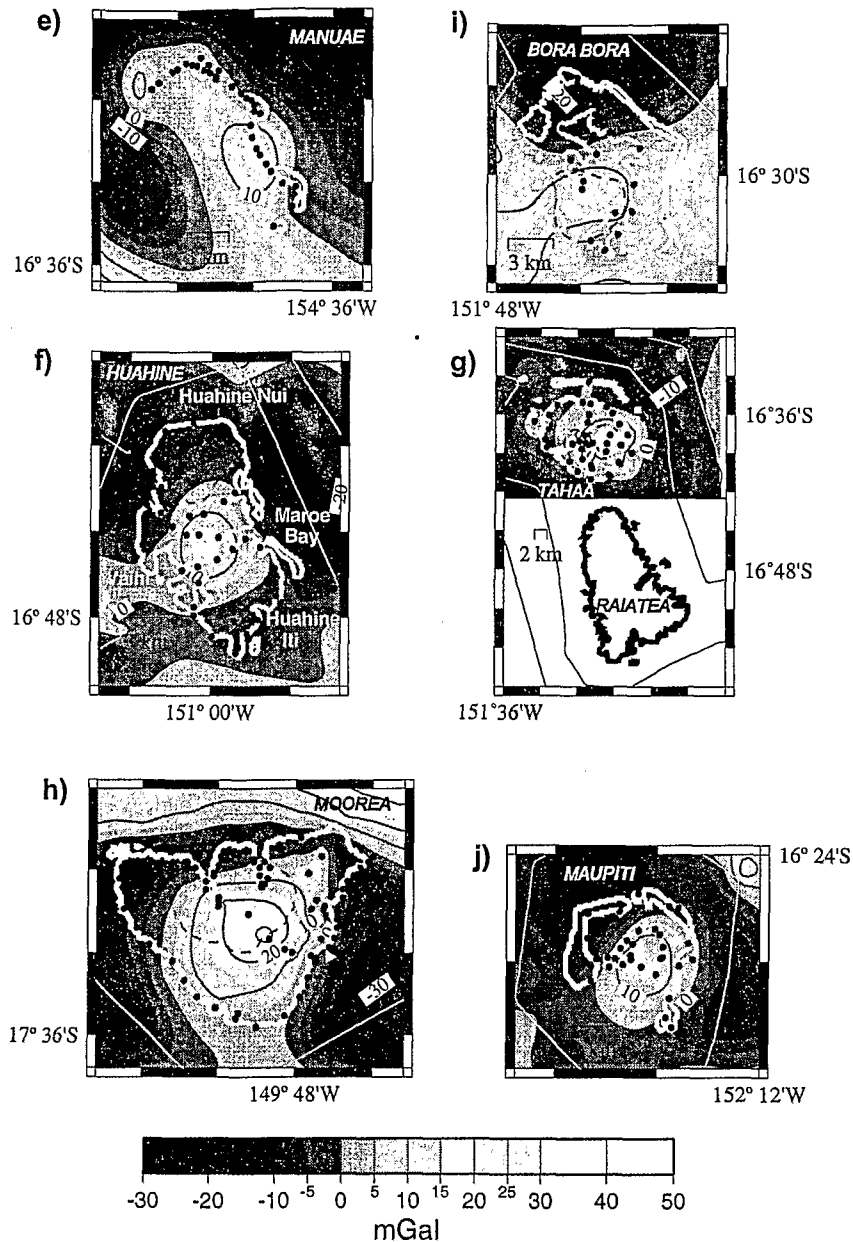
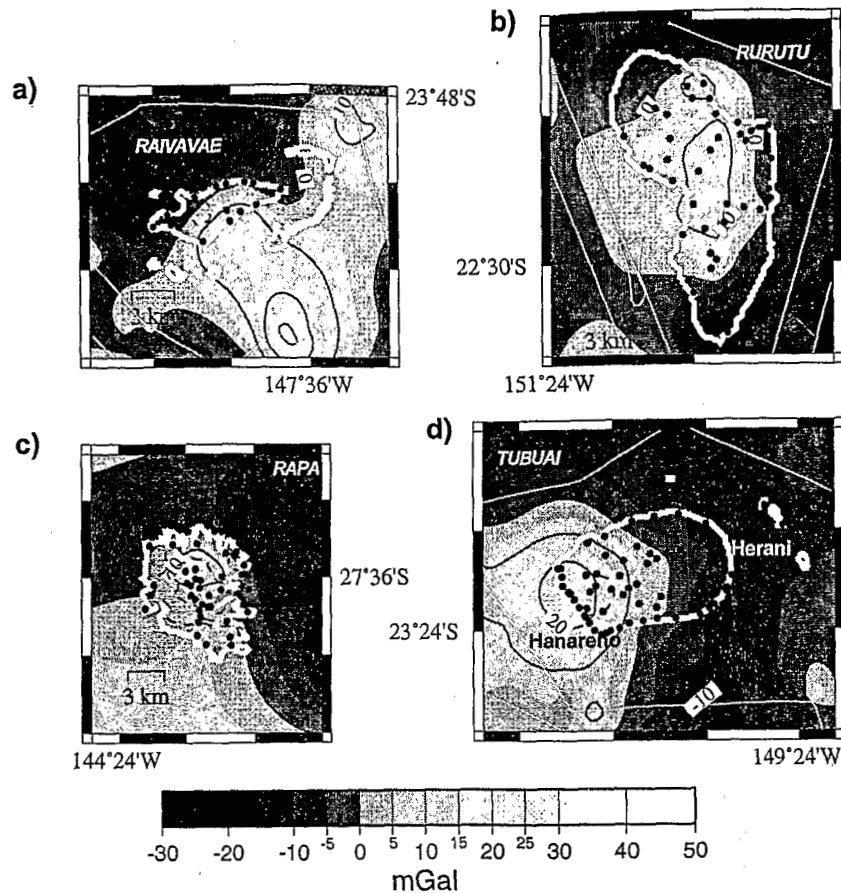


Figure 5. (continued)

is poor, except for its western part, where a prominent negative anomaly is observed. This negative anomaly is not consistent with the existence of a third and separate volcano as postulated by Léotot *et al.* [1990]. The negative anomaly of Tahiti Iti is discussed further below. The 10 mGal positive anomaly shown over the center of Tahiti Iti is not well constrained owing to the poor data coverage on the eastern shore of the peninsula and will not be considered further. On Manuae (Figure 5e) the anomaly is apparently located close to the eastern side of this atoll. However, since there are no data for the western and southern sides, the location of the anomaly is poorly defined.

Only one large positive anomaly is present over each island examined even though in some cases two dis-

tinct volcanoes have been postulated, such as on Tahiti Iti. There is some debate about Huahine (Figure 5f), which is composed of two separate islands located in the same lagoon (Huahine Nui and Huahine Iti), separated by Maroe Bay and a large intrusion at Mount Vaihi. Deneufbourg [1965] considers that these two islands are related to a single volcano separated by a large submerged caldera which formed Maroe Bay. In contrast, Brousse *et al.* [1983] postulate the presence of at least two volcanoes (Huahine Nui and Huahine Iti). Figure 5f clearly indicates one positive anomaly centered over Maroe Bay, which supports Deneufbourg's interpretation. A different interpretation may be appropriate in the case of the islands of Tahaa (Figure 5g) and Raiatea, which are in the same lagoon. Each island has



**Figure 6.** Isostatic residual anomaly over individual islands of the Austral Island chain where an anomaly greater than 5 mGal is observed. (a) Rapa, (b) Rurutu, (c) Tubuai, (d) Raivavae. Black dots represent land gravity stations, and black dashed lines represent caldera boundaries. Thick white lines represent the coast, and thin white lines represent the marine gravity data.

a caldera. The two calderas are separated by 25 km. Figure 5g shows a positive anomaly centered on the caldera of Tahaa. Unfortunately, no gravity survey has been conducted on Raiatea. However the gravity residual anomaly at Tahaa seems to show a separate feeding system.

Moorea (Figure 5h) has a 30 mGal anomaly, offset by about 3 km from the center of a caldera, while Bora Bora (Figure 5i) and Maupiti (Figure 5j) have 16 mGal and 18 mGal gravity anomalies, respectively, centered over associated calderas.

Thus each island in the Society chain apparently has only one deep-seated magma chamber or feeding system. Also, it is found that a linear correlation exists between the amplitude of the positive anomalies and the island size for both islands and atolls.

Negative anomalies (Table 3) are present over Tahiti Iti at Tairapu (Figure 5a) and Moorea (Figure 5g). On the basis of geological data [Léotot et al., 1990] those anomalies can be interpreted as the gravity effects of secondary cones producing differentiated lavas of relatively low density. A large volume of limestone deposits

could also have produced the observed negative anomaly on the coral reef of Bora Bora (Figure 5i).

### 3.2. Austral Islands

The Austral Islands chain extends northwest for > 1500 km from the active submarine volcano Macdonald [Norris and Johnson, 1969; Johnson and Malahoff, 1971; Talandier and Okal, 1984b] to the island of Rimatara, which is about 16 Myr old [Turner and Jarrard, 1982], and the atoll of Maria (Figure 1). The chain is composed of five small islands and one atoll. The age progression of these islands is compatible with a hot-spot origin, with the present volcanic activity related to the Macdonald submarine volcano [Duncan and McDougall, 1976]. Young radiometric ages reported for Rurutu, located toward the northern end of the chain, can be explained by another hotspot located between Rurutu and Tubuai [Turner and Jarrard, 1982]. The existence of this hotspot was established by demonstrating the differences of chemical and isotopic signatures of the recent lavas from Rurutu with those produced at the Macdonald hotspot [Barszczus et al., 1994]. Recent

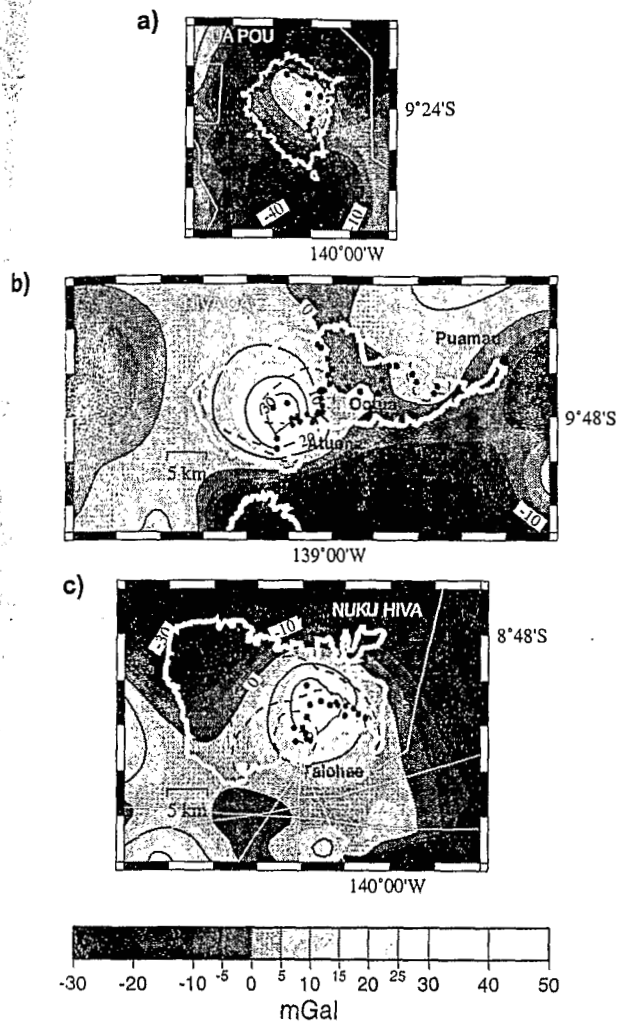


Figure 7. Isostatic residual anomaly over individual islands of the Marquesas Island chain: (a) Ua Pou, (b) Hiva Oa, (c) Nuku Hiva. Black dots represent land gravity stations, and black dashed lines represent caldera boundaries. Thick white lines represent the coast, and thin white lines represent the marine gravity data.

bathymetric and seismic data reported by *McNutt et al.* [1997] reveal the complexity of overlapping volcanism at the southeastern end of the Austral chain. The Austral FZ crosses the island chain between Tubuai and Raivavae, forming a western and eastern segment of the Austral island chain, each showing a distinct isotopic signature [*Barszczus et al.*, 1994; *Hauri et al.*, 1997]. The ages of the oceanic crust in the chain vary from about 35 Ma to 80 Ma [*Mayes et al.*, 1990].

Figure 6 shows the residual anomaly over the Austral Islands. Positive anomalies range from 16 mGal at Raivavae (Figure 6a) and Rurutu (Figure 6b) to 26 mGal at Tubuai (Figure 6c). Rapa (Figure 6d) presents a 17 mGal positive anomaly. These positive anomalies are interpreted as expressing a single and deep solidified magma chamber or feeding system. No significant anomalies are observed at Rimatara, the smallest and

northernmost island, and Maria, a small atoll located to the northwest of Rimatara.

The locations of the positive anomalies in the Austral Islands, like those in the Society Islands, are over the center of the island in Rapa and Rurutu but over the western shore in Tubuai and over the southern shore in Raivavae. The continuation of the anomaly to the south of Raivavae is probably due to a complex morphology of the southern submarine flank. The location and uniqueness of the gravity anomaly show a single magma source and imply that the so-called small caldera (see Figure 6d) is likely related to the collapse of

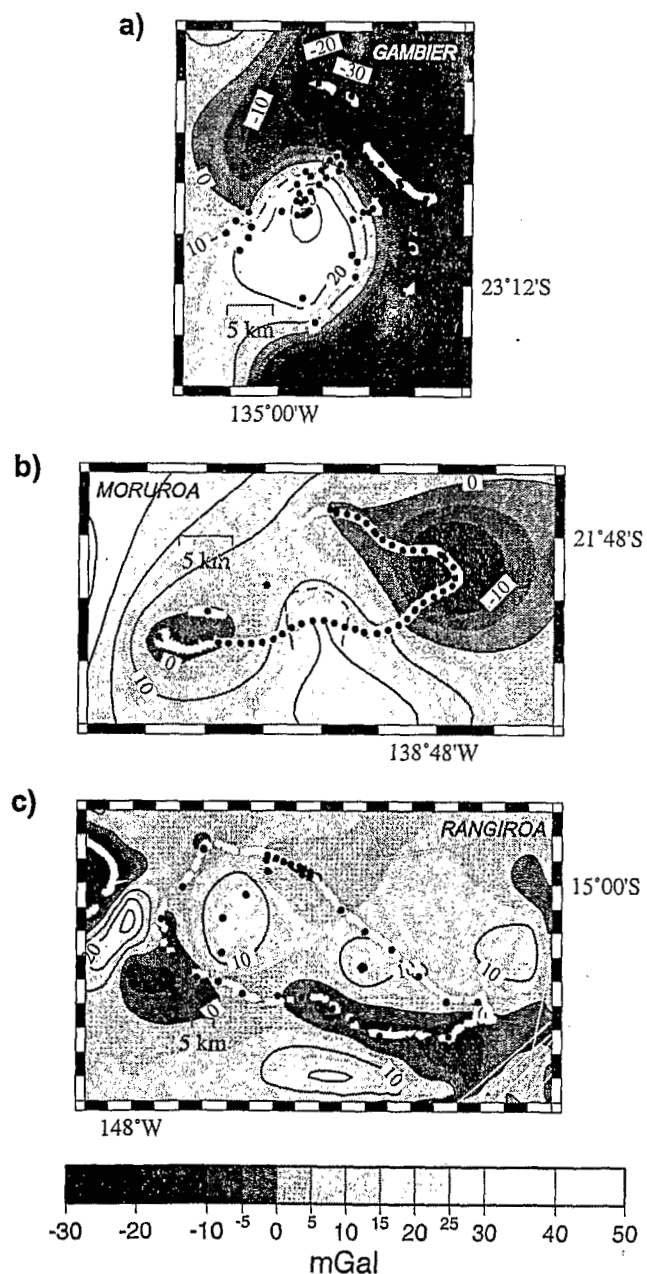


Figure 8. Isostatic residual anomaly over (a) Gambier Islands, (b) Moruroa, (c) Rangiroa. Black dots represent land gravity stations. Thick white lines represent the coast, and thin white lines represent the marine gravity data.

**Table 3.** Properties of Islands Showing Negative Residual Isostatic Anomalies

Island	Amplitude, mGal	Half Wavelength, km *	Location	Interpretation
Bora Bora	-20	4	north reef	low density superficial bodies
Moorea	-10	3	Maraarii secondary cone	differentiated lava
Nuku Hiva	-30	10	Topuke strombolian cone	differentiated lava
Tahiti Iti	-10	6.5	NW secondary cones	differentiated lava

\*The half wavelength represents the anomaly width.

the flanks of the volcano. On Tubuai the offset of the positive anomaly from the center of the island may indicate subsidence of this part of the island due to an underlying dense source (Figure 6c), similar to that observed in the Marquesas Islands [Chubb, 1930; Barszczus *et al.*, 1992]; the anomaly pattern strongly suggests the presence of a single magma source.

### 3.3. Marquesas Islands

The length of the Marquesas island chain is only 350 km, but it comprises a dozen islands and as many shallow seamounts. The age of the oceanic crust ranges from 50 to 55 Ma [Kruse, 1988; Mayes *et al.*, 1990; Munsch *et al.*, 1996]. K-Ar ages range from about 5.5 Ma at Eiao in the northwest to about 1.5 Ma at Fatu Iva in the southeast [Brousse *et al.*, 1990]. A basalt sample dredged 50 km southeast of Fatu Iva yielded an age of about 0.5 Ma [Desonie *et al.*, 1993]. The Marquesas FZ is located southeast of the chain. To date, no active hotspot generating the Marquesas volcanism has been identified.

Owing to the rugged topography, gravity stations are sparse (Figure 7), thus the resulting interpretations are somewhat speculative. The shipboard data coverage around the islands is also poor. The merging of these two poor data sets probably accounts for the non circular residual anomalies. The results for Ua Pou (Figure 7a) will not be considered further because of the poor distribution of data. Hiva Oa (Figure 7b) has a prominent positive anomaly (35 mGal) over the Atuona caldera. It is possible that a separate positive anomaly with a lower magnitude exists over the Puamau valley, but the lack of offshore data prevents any clear description of the anomaly. The observations at Hiva Oa indicate that at least one deep, solidified magma chamber is present at Hiva Oa. Obellianne [1955] proposed two calderas, Atuona and Puamau. These two calderas are separated by Mount Ootua, a trachytic diatreme, expressed as 5 mGal negative anomaly.

The anomaly pattern obtained at Nuku Hiva (Figure 7c) may be misleading because of the poor distribution of data. However, the positive anomaly (29 mGal) over the southern coast, where the data coverage is relatively good, may be associated with the caldera that forms Taiohae Bay.

### 3.4. Pitcairn-Gambier Islands

The Pitcairn-Gambier island chain extends over 1650 km from Hereheretue atoll to Pitcairn Island. Known K-Ar ages range from about 11 Ma at Moruroa [Guille *et al.*, 1993] to zero in the active hotspot area, 70 to 100 km southeast of Pitcairn [Binard *et al.*, 1992]. The Austral FZ crosses this chain between Moruroa and Fangataufa. The age of oceanic crust ranges from about 25 Ma in the southeast to 55 Ma to the northwest [Mayes *et al.*, 1990; Munsch *et al.*, 1996]. The chain includes the islands Pitcairn and the Gambier and several atolls. Fangataufa and Moruroa have been extensively drilled and thus considerable data on the properties and geology of these islands exist [see Guille *et al.*, 1993].

Over the Gambier Islands (Figure 8a), a large positive anomaly (34 mGal) occurs over the 10 islets in the center of a large lagoon. These islets are the emerged parts of an old volcano, and a caldera centered over the lagoon has been assumed [Guille, 1974]. The fist shape of the gravity anomaly is probably related to the lack of data in the lagoon, and the anomaly magnitude may actually be a few milliGals more than that indicated. Over the atoll of Moruroa (Figure 8b), a positive anomaly of 22 mGal is centered over the southern rim of the atoll. The positive gravity anomalies along the Pitcairn-Gambier island chain are interpreted as the remains of ancient magma chambers, which coincide with caldera locations for Moruroa [Buigues *et al.*, 1992], and for the Gambier Islands [Brousse *et al.*, 1972].

### 3.5. Tuamotu Islands

Oriented N120°, the Tuamotu Archipelago consists of about 60 atolls along two subparallel chains of length 1200 km and width 400 km. Its northern and southern termini are located at the Marquesas Fracture Zone and the Austral Fracture Zone, respectively. The age of the seafloor ranges from about 30 Ma in the southeast to 65 Ma in the northwest [Mayes *et al.*, 1990; Munsch *et al.*, 1996]. The atolls probably formed atop buried volcanoes.

Among the four atolls for which gravity data are available, only Rangiroa (Figure 8c) shows positive anomalies. The eastern anomaly (23 mGal) is only defined by one station and will not be considered further. By

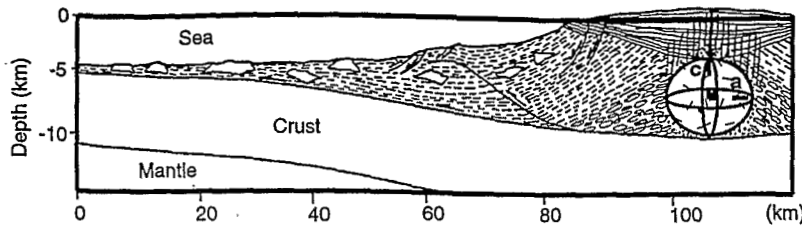


**Figure 9.** West-east cross section along latitude 19°06'N of Mauna Loa volcano, Hawai'i, extending from land to sea west-east [after Moore et al., 1995]. Horizontal layering indicates subaerial lava; dashed layering indicates fragmental lava; ellipses indicate pillow lava; vertical lines indicate sheeted dikes; dotted pattern indicates gabbro; unpatterned areas are giant blocks of first phase of South Kona landslide; and solid black areas are magma, or plastic core of southwest rift zone of Mauna Loa. The 3-D ellipsoidal chamber used to model the anomaly (see Figure 11) with a positive density contrast is also drawn.

analogy with results obtained for other islands (especially the Moruroa atoll) we interpret the western anomaly (17 mGal) as the gravity signature of an ancient magma chamber and/or deep-seated feeding system. It is possible that the amplitude of this anomaly could have been reduced due to the presence of a 2-km-thick coral limestone cap [Talandier and Okal, 1987] overlying the proposed magma chamber. For the three other, smaller atolls of Makatea, Manihi, and Mataiva (not shown), no appreciable anomaly is observed.

**4. Discussion**

Current understanding of volcanic edifices associated with hotspots and their tectonic behavior has been derived from numerous studies, mainly of the Hawaiian volcanoes. The first dynamic cross section of a typical

Hawaiian volcano [Eaton and Murata, 1960] proposed that the magma ascends (due to buoyancy) to a depth between 3 and 7 km, where it forms a shallow magma reservoir. Intermittent eruptions occur within summit calderas or laterally along rift zones. Ryan [1987] formulated the neutral buoyancy hypothesis in which the magma ascends to depths where its density equals that of the surrounding material. This region of neutral buoyancy controls the upper limit of the levels of stable magma storage. The summit reservoir elevation follows the buildup of the volcano, leading to the location of the roof at depths between 2 and 4 km, as observed on Kilauea and Mauna Loa volcanoes (Figure 9) [Moore et al., 1995]. Another characteristic of hotspot volcanoes is the existence of collapses. The Hawaiian Ridge is characterized by giant submarine landslide debris, which played a key role in the internal makeup of the

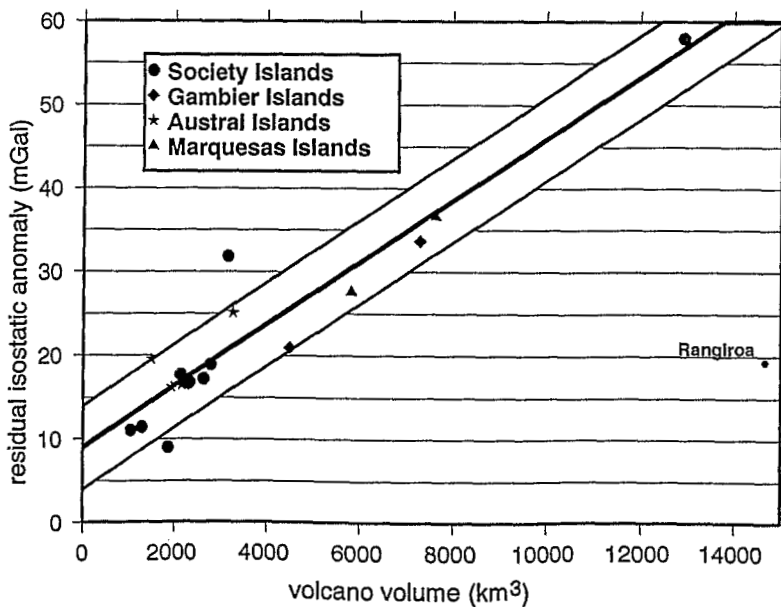


**Figure 10.** Plot of the maximum intensity of the positive residual anomaly (mGal) versus island volume (km<sup>3</sup>). Shaded area represents the  $\pm 5$  mGal error associated with the observed gravity values. The central thick line represents the derived linear relation between volcano volume and anomaly amplitude.



volcanoes [Moore *et al.*, 1989]. These landslides can have various origins [e.g., Walker, 1988]: vertical subsidence by withdrawal of magma beneath the summit area or lateral mass collapse. Using our gravity data set, we will try to compare the Polynesian volcanoes to this classical Hawaiian model.

#### 4.1. Gravity Anomalies

Positive residual gravity anomalies are calculated over 20 islands, with amplitudes ranging from 9 to 60 mGal (Table 2). Generally, the anomalies are spatially correlated with a known caldera (e.g., Tahiti) or the assumed main feeding conduit of volcanoes of similar widths. Thus solidified magma chambers and feeding conduits with higher densities than that of the surrounding rocks [Rymer and Brown, 1986; Rousset *et al.*, 1989] produce the observed positive gravity anomalies. Furthermore, for each island where the gravity coverage is good the observed single positive anomaly suggests that there is only one deep-seated, solidified magma chamber or main feeding system.

We also observe a good correlation (Figure 10) between the amplitude of the positive anomaly and the volume of the volcano. This volume is that bounded by the volcano topography and a reference plane corresponding to the observed basis of the volcano on the seafloor. Specifically, the linear relation between the volcano volume  $V_v$  and the amplitude of the positive anomaly  $A_p$  is

$$A_p = 3.7 \times 10^{-3} V_v + 8.9, \quad (3)$$

where  $V_v$  is in  $\text{km}^3$  and  $A_p$  is in mGal. This relation fails for the Rangiroa atoll, however, where the gravity signal is lower than expected considering the volcano diameter. It has already been pointed out that the amplitude of the gravity anomaly at Rangiroa may have been reduced due to a 2 km-thick coral limestone cap. Thus the volcanic basement and the dense residue of magmatic rock are located at a greater depth than that for the other islands.

Negative anomalies (Table 3) are observed in a few cases, although their magnitude never reaches that of the positive anomalies. Moreover, in contrast to the positive anomalies, the negative anomalies are observed on the island or atoll edge, possibly because of limestone on reefs or fragmented material on the flank of the edifices.

#### 4.2. Size and Depth of Solidified Magma Chambers

Residual gravity anomalies are associated with shallow mass inhomogeneities. Robertson [1967] tried to model the gravity anomalies observed on six of the Cook Islands as caused by vertical cylindrical dense cores with a radius equal to the radius of the island at sea level. Despite the simplicity of the model, which uses a uniform density for the whole island, Robertson found a

single relation between the size of the solidified magma plumbing system and the present size of the volcano. Using a more realistic model, we examine usefulness of this relation.

In most cases, the amplitudes of the gravity anomalies are based on a single profile across the island. The anomaly can be modeled, in a simple way, as the effect of a dense ellipsoid of revolution (Figure 11). More sophisticated inverse or forward models would be uninformative in the absence of any other data constraints, such as seismic or borehole data. The selected ellipsoidal body does not reflect the complexity of magma reservoirs and feeding conduits. Nevertheless, it is a reasonable representation of the depth and volume of the main system. Using this simple approach of an ellipsoidal magma chamber, the radius, the flattening, and the depth of the chamber of each island can be derived as a function of the residual anomaly. At a point  $P$  located at a distance  $r$  from the center of the ellipsoid the vertical attraction  $g_v$  of an ellipsoid of revolution is

$$g_v = \frac{4\pi a^2 c G \Delta \rho z}{3(r^2 + z^2)^{3/2}} \left[ 1 - \frac{3(a^2 - c^2)(2z^2 - r^2)}{10(r^2 + z^2)^2} \right] \quad (4)$$

where  $z$  is the depth of the center of the ellipsoid,  $2a$  is the diameter of the circular section of the ellipsoid,  $c$  is the length of the vertical axis of revolution (see Figure 9),  $\Delta \rho$  is the density contrast, and  $G$  is the gravitational constant ( $6.67 \times 10^{-11}$  N m). The average density for ultramafic bodies forming dense magma chambers or feeding systems is roughly  $3100\text{--}3300 \text{ kg m}^{-3}$  [Rymer and Brown, 1986]: we used a value of  $3100 \text{ kg m}^{-3}$ . The density contrast  $\Delta \rho$  depends on the submarine load density  $\rho_s$  assumed for each island, except for Rangiroa, where we set  $\Delta \rho$  to  $500 \text{ kg m}^{-3}$ . To constrain our results further, we also assume that the magma chamber depth lies between 2 and 4 km, the depth of neutral buoyancy [Ryan, 1987]. Considering that the islands have reached an elevation of 2000 m above sea level, the magma chamber would lie at depth of 0 m to 2 km below the sea level. Although the neutral buoyancy region has been defined for active volcanoes, we have assumed it applies here because of the young ages of the volcanoes in our study area (except Rangiroa). The final parameters of the ellipsoids,  $a$ ,  $c$  and  $z$ , are those that minimize the difference between the isostatic residual anomalies and the attraction of the ellipsoidal body given by equation (4).

For each island, Table 4 gives the diameter and the depth of the magma chamber roof. For the Society Islands the magma chamber roof depth varies from 100 m for Maiao, Maupiti, Moorea and Tupai to 1.3 km for Tahiti. The diameter of the chamber ranges from 2 km for Maiao to 14 km for Tahiti. For the Austral Islands the sizes of chamber range from 3.6 to 7 km. The Gambier Islands, Rangiroa, and Marquesas islands generally have larger magma chambers (from 8.4 to 11.6 km in diameter) lying at greater depths (up to 5.9 km). Plot-

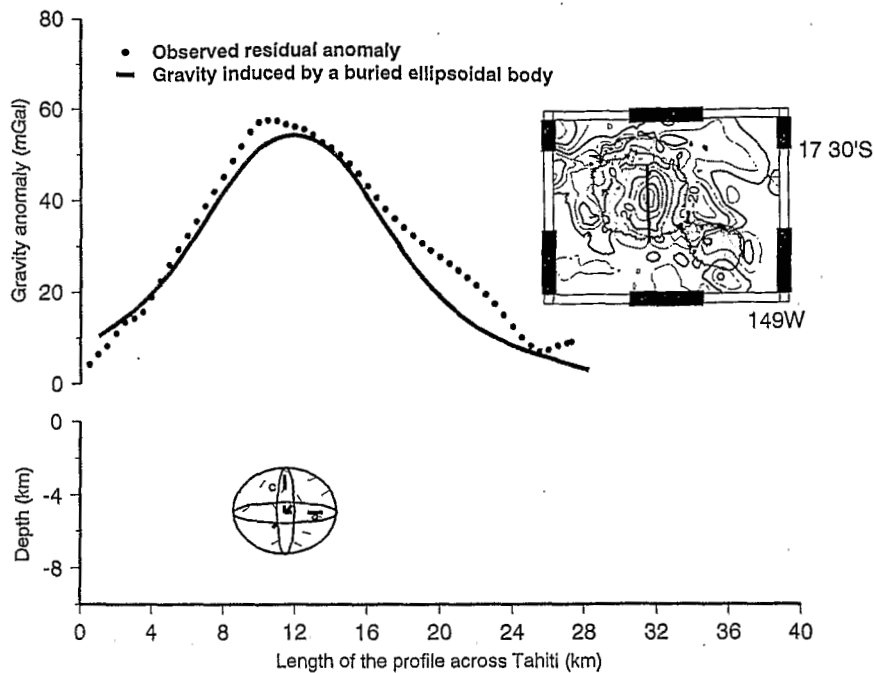


**Figure 11.** Gravity anomaly produced by a 3-D ellipsoidal chamber with a positive density contrast (see text) with the surrounding rocks on Tahiti. The isostatic residual anomaly in milliGals is represented as a dotted line, and the computed anomaly is represented as a solid line. The inset shows the location of the profile on Tahiti Island.

ting the magma chamber volume  $V_m$  ( $\text{km}^3$ ) versus the volcano volume  $V_v$  ( $\text{km}^3$ ) (Figure 12) gives the following linear relation:

$$V_m = 7.14 \times 10^{-2} V_v - 91. \quad (5)$$

This relation gives a method to infer the rough size of the solidified magma chamber using only the volcano volume. To compare with other intraplate volcanoes, we plotted data from the Kilauea [Ryan, 1988] and Piton des Neiges [Lesquer, 1990] volcanoes. Although the size of these volcanoes is difficult to estimate since they can not be easily separated from other nearby volcanoes, the Piton des Neiges point on the graph fits well with the linear curve determined for the islands of French Polynesia. The proposed relation in equation (5) does not apply for Kilauea, probably because the volume of this volcano is very difficult to estimate. Therefore our method probably applies only to extinct volcanoes and thus entirely solidified magma chambers.

### 4.3. Load Density

On a regional scale a submarine volcanic load density of  $2700 \text{ kg m}^{-3}$  provides reasonable results for the calculated deflection surface and for the theoretical FAA (Figure 4). This value may thus suitably represent the actual average regional load density for volcanic island chains. For individual islands, however, the RMS error between theoretical and observed FAA leads to a range of submarine load densities, from  $2300$  to  $2900 \text{ kg m}^{-3}$

for all the islands (Table 2). On this local scale the density of the masses above sea level has a major effect on the terrain correction. An average value of  $2300 \text{ kg m}^{-3}$  for  $\rho_a$ , the density of the aerial part of the islands, provides suitable results for all the islands. The value of the filling density  $\rho_f$  was determined jointly by the same RMS minimization method and varies from

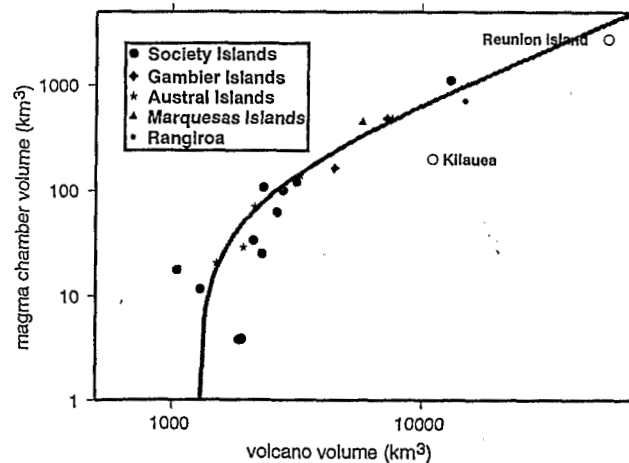


**Figure 12.** Computed solidified magma chamber volume versus the island volume using a logarithmic representation. The trend of the plot in gray corresponds to a linear relation. French Polynesian volcanoes are represented by solid geometrical symbols (see legend), and volcanoes from Hawai'i and Reunion Islands are plotted for comparison using open circles.

Table 4. Characteristics of Magma Chambers and Comparison With the Size of the Caldera

Island	Caldera		Solidified Magma Chamber ( $\rho = 3100 \text{ kg m}^{-3}$ )				
	Diameter, km	Center Longitude W	Center Latitude S	Diameter $a$ , km	Flattening $c/a$	Volume, $\text{km}^3$	Roof Depth, km
Austral							
Raivavae	3	147°39'	23°53'	5.4	0.85	70	0.2
Rapa	3.5 and 5	144°21'	27°36'	3.6	0.83	20	0.2
Rurutu	...	152°21'	22°29'	3.8	1.0	29	0.1
Tubuai	2	149°31'	23°23'	7.0	0.77	138	0.2
Marquesas							
Hiva Oa	10 and 15	139°03'	09°48'	8.4	1.52	473	0.3
Nuku Hiva	6 and 9	140°06'	08°54'	8.4	1.43	443	0.2
Society							
Bora Bora	4	151°45'	16°31'	6.4	0.78	107	0.2
Huahine	...	151°00'	16°46'	5.2	0.85	62	0.3
Maiao	...	150°37'	17°40'	2.0	0.9	4	0.1
Manuae*	...	154°39'	16°32'	4.0	0.75	25	0.3
Maupiti	3	152°16'	16°27'	4.0	1.0	33	0.1
Moorea	7	149°49'	17°32'	6.2	0.97	121	0.1
Tahaa	4	151°28'	16°38'	6.2	0.81	101	0.8
Tahiti	7	149°26'	17°38'	14.0	0.77	1108	1.3
Tetiaroa	...	149°34'	17°01'	2.8	1.0	12	0.3
Tupai	...	151°49'	16°16'	3.6	0.72	18	0.1
Tuamotu-Gambier							
Gambier	12	134°58'	23°09'	9.6	1.04	482	1.6
Moruroa	...	138°54'	21°52'	7.2	0.83	163	1.8
Rangiroa	...	147°48'	15°05'	11.6	0.86	705	5.9

\*Poorly constrained.

2800 to 2900  $\text{kg m}^{-3}$ , except for Moruroa and Rangiroa, where it is lower.

#### 4.4. Calderas or Collapses?

Are the computed locations and diameters of the ancient magma chambers consistent with those of known calderas? It appears that the collapse diameter is sometimes larger than the computed diameter of the associated magma chamber. In addition, the collapses are not always located directly above the chambers themselves (e.g., north of Huahine). Considering the inferred magma chamber location, the collapse of Tahaa is shifted west, that of Moorea is shifted north, and those of Huahine and Raivavae are clearly independent of the location of the magma chamber. Hiva Oa, Nuku Hiva, and Rapa have outer collapses larger than the proposed solidified reservoirs. These collapses are probably not linked to any caldera subsidence but rather to flank instabilities (e.g., landslides) such as described on other intraplate volcanoes such as Hawaii or Reunion islands [Moore et al., 1989; Lénat and Labazuy, 1990]. However, inner collapses of Rapa and Hiva Oa, the eastern collapse of Tahaa, and the collapses of Gambier Islands,

Tubuai, Maupiti, Tahiti Nui, and Bora Bora are probably characterized by classic calderas centered above the magma chamber. Even for these edifices, however, the caldera flank is always open to the sea, and this could be related to flank instabilities.

#### 5. Conclusion

A gravity study of 25 volcanic islands in French Polynesia leads us to propose a single linear relation between the island size and the solidified magma chamber size, the latter being derived from the positive isostatic residual gravity anomaly. This linear relation appears appropriate for other hotspot volcanoes, such as Piton des Neiges in Reunion Island. This relation may be used as a simple and viable tool to infer the rough size of the solidified magmatic feeding system for extinct oceanic intraplate volcano.

The results also illustrate the wide range of submarine volcanic load densities, from 2300 to 2900  $\text{kg m}^{-3}$ , and confirm the importance of the increase of density with depth, from 2300  $\text{kg m}^{-3}$  for subaerial lava to 2900  $\text{kg m}^{-3}$  for the deepest part of the volcano which fills

the flexure of the oceanic crust. On a regional scale the best fitting load density is  $\sim 2700 \text{ kg m}^{-3}$ .

At the island scale the residual isostatic anomaly helps to define the actual location of volcanoes. For example, previous studies assume multiple volcanoes on the same island (e.g., Huahine, Tubuai, Tahiti Iti). However, our results clearly demonstrate the presence of a single volcanic system for these islands and for the atolls, except for the Marquesas Islands. Finally, we show that the majority of the so-called calderas are related to flank instabilities which induce huge landslides, rather than to caldera subsidence. Thus the caldera center may often be a poor indicator of the locations and other attributes of now consolidated and inactive ancient magma reservoirs.

**Acknowledgments.** We are grateful for ORSTOM institute, now IRD, that funded all the gravity surveys conducted by one of us (H.G.B.) in French Polynesia between 1978 and 1981 and to I. Leroy who made the complete gravity survey of Tahiti in 1994. V.C. is supported by a grant of the ZEPOLYF program. We thank particularly the associate editor, T. Hildenbrand, whose remarks and suggestions have greatly improved this paper. This work also benefited of the constructive reviews made by J.F. Lénat, M.P. Ryan, and H. Rymer.

## References

- Barriot, J.P., La détermination du géoïde par altimétrie océanique et gravimétrie : Quelques aspects du traitement et interprétation géologique sur l'Océan Indien (partie NO) et Méditerranée occidentale. Ph.D. thesis, 240 pp, Univ. des Sciences et Techniques du Languedoc, Montpellier, France, 1987.
- Barszczus, H.G., Résultats provisoires de quelques mesures et liaisons gravimétriques effectuées en Polynésie Française, *Intern. Rep., Cent. ORSTOM de Papeete, Tahiti*, 1979.
- Barszczus, H.G., Reconnaissance gravimétrique de Tubuai (Iles Australes), *Intern. Rep., Cent. ORSTOM de Papeete, Tahiti*, 1980.
- Barszczus, H.G., Reconnaissance gravimétrique de Maïao (Tupai-Manu), *Intern. Rep., Cent. ORSTOM de Papeete, Tahiti*, 1981.
- Barszczus, H.G., P.E. Filmer, and D.L. Desonie, Cataclysmic collapses and mass wasting processes in the Marquesas (abstract), *Eos Trans. AGU*, 73 (14), Spring Meet. Suppl., 313, 1992.
- Barszczus, H.G., G. Guille, R.C. Maury, C. Chauvel, and H. Guillou, Two magmatic sources at Rurutu Island (Austral Islands, French Polynesia) and the Austral "Hotline" (abstract), *Eos Trans. AGU*, 75(44), Fall Meet. Suppl., 323, 1994.
- Binard, N., R. Hékinian, J.L. Cheminée, R.C. Searle, and P. Stoffers, Morphological and structural studies of the Society and Austral hot spot regions in the South Pacific, *Tectonophysics*, 186, 293-312, 1991.
- Binard, N., R. Hékinian, and P. Stoffers, Morphostructural study and type of volcanism of submarine volcanoes over the Pitcairn hotspot in the South Pacific, *Tectonophysics*, 206, 245-264, 1992.
- Blakely, R.J., *Potential Theory in Gravity and Magnetic Applications*, 441 pp., Cambridge Univ. Press, New York, 1995.
- Bonneville, A., V. Clouard, P. Beuzart, I. Klaucke, R. Le Suavé, B. Loubrieu, P. Saget, and Y. Thomas, Possible control of Society Islands volcanism by a preexisting volcanic chain (abstract), *Eos Trans. AGU*, 78(45), Fall Meet. Suppl., F725, 1997.
- Brousse, R., J.C. Philippet, G. Guille, and H. Bellon, Géochronométrie des îles Gambier (Océan Pacifique), *C. R. Acad. Sci., Ser. D*, 274, 1995-1998, 1972.
- Brousse, R., C. Macherey, E. Berger, and G. Bontault, L'île de Huahine: trois volcans successifs (Archipel de la Société, Polynésie), *C. R. Acad. Sci., Ser. II*, 296, 1559-1562, 1983.
- Brousse, R., H.G. Barszczus, H. Bellon, J.M. Cantagrel, C. Diraison, H. Guillou, and C. Léotot, Les Marqueses (Polynésie Française): Volcanologie, géochronologie, discussion d'un modèle de point chaud, *Bull. Soc. Géol. Fr.*, 6, 933-949, 1990.
- Buigues, D., A. Gachon, and G. Guille, L'atoll de Moruroa (Polynésie Française): Structure et évolution géologique, *Bull. Soc. Géol. Fr.*, 5, 645-657, 1992.
- Calmant, S., and A. Cazenave, The effective elastic lithosphere under the Cook Austral and Society Islands, *Earth Planet. Sci. Lett.*, 77, 187-202, 1986.
- Calmant, S., and A. Cazenave, Anomalous elastic thickness of the oceanic lithosphere in the south central Pacific, *Nature*, 328, 236-238, 1987.
- Cares, D.W., M.K. McNutt, R.C. Detrick, and J.C. Mutter, Seismic imaging of hotspot-related crustal underplating beneath the Marquesas Islands, *Nature*, 373, 600, 1995.
- Cheminée, J.L., R. Hékinian, J. Talandier, F. Albarède, C.W. Devey, J. Francheteau, and Y. Lancelot, Campagne Teahitia-1, Géologie d'un point chaud actif: Teahitia-Mehetia, îles de la Société (Pacifique Central Sud), *Oceanol. Acta*, 10, 225-239, 1990.
- Chubb, L.J., The geology of the Marquesas Islands, *Bull. 68*, B.P. Bishop Mus., Honolulu, Hawaii, 1930.
- Dalrymple, G.B., R.D. Jarrard, and D.A. Clague, Potassium-argon ages of some volcanic rocks from the Cook and Austral Islands, *Geol. Soc. Am. Bull.*, 86, 1463-1467, 1975.
- Danobeitia, J.J., et al., Deep seismic reconnaissance beneath Society Archipelago (South Pacific), paper presented at EGS Assembly, Eur. Geophys. Soc., Hamburg, Germany, 1995.
- Deneufbourg, G., Carte géologique, Notice explicative sur la feuille Huahine, *Bur. des Rec. Géol. et Minièr., Paris*, 1965.
- Desonie, D. L., R.A. Duncan, and J.H. Natland, Temporal and geochemical variability of volcanic products of the Marquesas hotspot, *J. Geophys. Res.*, 98, 17,649-17,665, 1993.
- Diraison, C., Le volcanisme aérien des archipels polynésiens de la Société, des Marqueses et des Australes-Cook, Ph.D. thesis, 413 pp, Univ. de Bretagne Occidentale, Brest, France, 1991.
- Diraison, C., H. Bellon, C. Léotot, R. Brousse, and H. Barszczus, L'alignement de la Société (Polynésie française): Volcanologie, géochronologie, proposition d'un modèle de point chaud, *Bull. Soc. Géol. Fr.*, 162, 479-496, 1991.
- Duncan, R.A., and I. McDougall, Migration of volcanism with time in the Marquesas Islands, French Polynesia, *Earth Planet. Sci. Lett.*, 21, 414-420, 1974.
- Duncan, R.A., and I. McDougall, Linear volcanism in French Polynesia, *J. Volcanol. Geotherm. Res.*, 1(3), 197-227, 1976.
- Duncan, R.A., M.R. Fisk, W.M. White, and R.L. Nielsen, Tahiti: Geochemical evolution of a French Polynesian volcano, *J. Geophys. Res.*, 99, 24,341-24,357, 1994.
- Eaton, J.P., and K.J. Murata, How volcanoes grow, *Science*, 132, 925-938, 1960.
- Filmer, P.E., Flexure of the oceanic lithosphere in the vicinity

- ity of the Marquesas Islands, Ph.D. thesis, 234 pp, Mass. Inst. of Technol., Cambridge, 1991.
- Filmer, P.E., M.K. McNutt, and C.J. Wolfe, Elastic thickness of the lithosphere in the Marquesas and Society Islands, *J. Geophys. Res.*, **98**, 19,565-19,577, 1993.
- Gillot, P.Y., Y. Cornette, and G. Guille, Age (K-Ar) et conditions d'édification du soubassement volcanique de l'atoll de Moruroa (Pacifique Sud), *C. R. Acad. Sci., Ser. II*, **314**, 393-399, 1992.
- Goodwillie, A.M., and A.B. Watts, An altimetric and bathymetric study of elastic thickness in the central Pacific Ocean, *Earth Planet. Sci. Lett.*, **118**, 311-326, 1993.
- Guille, G., Contribution à l'étude géologique des îles de Polynésie française: Les Gambiers, Ph.D. thesis, 215 pp, Univ. Paris XI, Orsay, France, 1974.
- Guille, G., R.C. Maury, D. Buigues, H. Bellon, A. Gachon, and M. Caroff, L'Atoll de Moruroa (Polynésie française); III, Conclusions générales, *Bull. Soc. Geol. Fr.*, **163**, 681-685, 1992.
- Guille, G., G. Goutière, and J.F. Sornein, *Les atolls de Mururoa et de Fangataufa (Polynésie Française)*, vol. I. *Géologie, Pétrologie, Hydrogéologie*, 168 pp., Masson, Paris, 1993.
- Guillou, H., P.Y. Gillot, and G. Guille, Age (K-Ar) et position des îles Gambier dans l'alignement du point chaud de Pitcairn (Pacifique Sud), *C. R. Acad. Sci., Ser. II*, **318**, 635-641, 1994.
- Hauri, E.H., J.C. Lassiter, and H.G. Barszczus, Lithospheric controls on the compositions of Austral Islands lavas: Isotopic evidence from Raivavae and the southern Australs (abstract), *Eos Trans. AGU*, **78**(46), Fall Meet. Suppl., F828, 1997.
- Herron, E.M., Sea-floor spreading and the cenozoic history of the east-central Pacific, *Geol. Soc. Am. Bull.*, **83**, 1671-1692, 1972.
- Ito, G., M. McNutt, and R.L. Gibson, Crustal structure of the Tuamotu Plateau, 15°S, implications for its origin, *J. Geophys. Res.*, **100**, 8097-8114, 1995.
- Johnson, R.H., and A. Mahaloff, Relation of Macdonald volcano to migration of volcanism along the Austral chain, *J. Geophys. Res.*, **76**, 3282-3290, 1971.
- Krummenacher, D., and J. Noetzelin, Datations de coulées éruptives dans différents archipels de la Polynésie Française, *Bull. Soc. Geol. Fr.*, **3**, 131, 1966.
- Kruse, S.E., Magnetic lineations on the flanks of the Marquesas swell: Implications for the age of the seafloor, *Geophys. Res. Lett.*, **15**, 573-576, 1988.
- Lénat, J.F., and P. Labazuy, Submarine morphologies and structures of Reunion, in *Le Volcanisme de la Réunion-Monographie*, edited by J.F. Lénat, pp. 43-74, Cent. Rech. Volcanol., Clermont-Ferrand, France, 1990.
- Léotot, C., P.Y. Gillot, F. Guichard, and R. Brousse, Le volcan de Taravao (Tahiti): Un exemple de volcanisme polyphasique associé à une structure d'effondrement, *Bull. Soc. Geol. Fr.*, **6**, 951-961, 1990.
- Leroy, I., Evolution des volcans en système de point chaud: Ile de Tahiti, archipel de la Société (Polynésie Française), Ph.D. thesis, 271 pp, Univ. Paris XI, Orsay, France, 1994.
- Lesquer, A., Deep structure of Reunion Island from gravity data, in *Le volcanisme de la Réunion-Monographie*, edited by J.F. Lénat, pp 19-27, Cent. Rech. Volcanol., Clermont-Ferrand, France, 1990.
- Macheski, L.F., Gravity relations in American Samoa and the Society Islands, *Pacific Sci.*, **19**, 367-373, 1965.
- Mammerickx, J., E. Herron, and L. Dorman, Evidence for two fossil spreading ridges in the southeast Pacific, *Geol. Soc. Am. Bull.*, **91**, 263-271, 1980.
- Mayes, C.L., L.A. Lawver, and D.T. Sandwell, Tectonic history and new isochron chart of the south Pacific, *J. Geophys. Res.*, **95** 8543-8567, 1990.
- McNutt, M.K., Lithospheric flexure and thermal anomalies, *J. Geophys. Res.*, **89**, 11,180-11,194, 1984.
- McNutt, M.K., Superswells, *Rev. Geophys.*, **36**(2), 211-244, 1998.
- McNutt, M.K., D.W. Caress, J. Reynolds, K.A. Jordahl, and R.A. Duncan, Failure of plume theory to explain midplate volcanism in the southern Austral islands, *Nature*, **389**, 479-482, 1997.
- Minster, J.B., and T.G. Jordan, Present-day plate motions, *J. Geophys. Res.*, **83**, 5331-5354, 1978.
- Moore, J.G., D.A. Clague, R.T. Holcomb, P.W. Lipman, W.R. Normark, and M.E. Torresan, Prodigious submarine landslides on the Hawaiian ridge, *J. Geophys. Res.*, **94**, 17,465-17,484, 1989.
- Moore, J.G., W.B. Bryan, M.H. Besson, and W.R. Normark, Giant blocks in the South Kona landslide, Hawaii, *Geology*, **23**, 125-128, 1995.
- Munsch, M., C. Antoine, and A. Gachon, Evolution tectonique de la région des Tuamotu, océan Pacifique central, *C. R. Acad. Sci., Ser. II*, **323**, 941-948, 1996.
- Nakagawa, I., et al., Precise calibration of scale values of Lacoste & Romberg gravimeters and international gravimetric connections along the circum-Pacific zone, *Tech. Rep. Kyoto Univ.*, Kyoto, Japan, 1983.
- Norris, A., and R.H. Johnson, Submarine volcanic eruptions recently located in the Pacific by SOFAR hydrophones, *J. Geophys. Res.*, **74**, 650-664, 1969.
- Obellianne, J.M., Contribution à l'étude géologique des îles des Etablissements Français de l'Océanie. *Sci. Terre*, **3**, 1-146, 1955.
- Okal, E.A., and A. Cazenave, A model for the plate tectonic evolution of the east-central Pacific based on Seasat investigations, *Earth Planet. Sci. Lett.*, **72**, 99-116, 1985.
- ORSTOM, Atlas de la Polynésie Française, Paris, 1993.
- Pautot, G., Analyse structurale de l'archipel des Tuamotu: Origine volcano-tectonique, paper presented at 3ème Colloque des Sciences de la Terre, Univ. Montpellier, Montpellier, France, 1975.
- Plouff, D., Gravity and magnetic fields of polygonal prisms and application to magnetic terrain corrections, *Geophysics*, **41** (4), 727-741, 1976.
- Robertson, E.I., Gravity effects of volcanic islands, *N. Z. J. Geol. Geophys.*, **10**(6), 1466-1483, 1967.
- Rousset, D., A. Lesquer, A. Bonneville, and J.F. Lénat, Complete gravity study of Piton de la Fournaise volcano, Reunion Island, *J. Volcanol. Geotherm. Res.*, **36**, 37-52, 1989.
- Ryan, M.P., Neutral buoyancy and the mechanical evolution of magmatic systems, in *Magmatic Processes: Physicochemical Principles*, edited by B.O. Mysen, Geoch. Soc. Spec. Pub. 1, 259-287, 1987.
- Ryan, M.P., The mechanics and three-dimensional internal structure of active magmatic systems: Kilauea Volcano, Hawaii, *J. Geophys. Res.*, **93**, 4213-4248, 1988.
- Rymer, H. and G.C. Brown, Gravity fields and the interpretation of volcanic structures: Geological discrimination and temporal evolution, *J. Volcano. Geotherm. Res.*, **27**, 229-254, 1986.
- Sandwell, D.T., Antarctic marine gravity field from high-density satellite altimetry, *Geophys. J. Int.*, **109**, 437-448, 1992.
- Service de l'Urbanisme, Carte topographique 1:20,000, Paapeete, Tahiti, French Polynesia, 1992.
- Sichoix, L., Le volcanisme de Polynésie Française: Caractérisation des points chauds et du superbombement

- à partir d'une nouvelle synthèse bathymétrique, Ph.D. thesis, 297 pp, Univ. Fr. du Pac., Papeete, Tahiti, 1997.
- Sichoix, L., and A. Bonneville, Prediction of bathymetry in French Polynesia constrained by shipboard data. *Geophys. Res. Lett.*, **23**, 2469-2472, 1996.
- Smith, W.H.P., On the accuracy of digital bathymetric data, *J. Geophys. Res.*, **98**, 9591-9603, 1993.
- Smith, W.H.P., and D.T. Sandwell, Marine gravity field from declassified Geosat and ERS-1 altimetry (abstract), *Eos Trans. AGU*, **76** (46), Fall Meet. Suppl., F156, 1995.
- Smith, W.H.P., and P. Wessel, Gridding with continuous curvature splines in tension, *Geophysics*, **55**, 293-305, 1990.
- Talandier, J., and E.A. Okal, The volcanoseismic swarms of 1981-1983 in the Tahiti-Mehetia area, French Polynesia, *J. Geophys. Res.*, **89**, 11,216-11,234, 1984a.
- Talandier, J., and E.A. Okal, New surveys of Macdonald seamount, southcentral Pacific, following volcanoseismic activity, 1977-1983, *Geophys. Res. Lett.*, **11**, 813-816, 1984b.
- Talandier, J., and E.A. Okal, Crustal structure in the Society and Tuamotu Islands, French Polynesia, *Geophys. J. R. Astron. Soc.*, **88**, 499-528, 1987.
- Turner, D.L., and R.D. Jarrard, K-Ar dating of the Cook-Austral island chain: A test of the hot spot hypothesis, *J. Volcano. Geotherm. Res.*, **12**, 187-220, 1982.
- Walcott, R.I., Flexure of the lithosphere at Hawaii, *Tectonophysics*, **9**, 435-446, 1970.
- Walker, G.P.L., Three Hawaiian calderas: An origin through loading by shallow intrusions?, *J. Geophys. Res.*, **93**, 14,773-14,784, 1988.
- Watts, A.B., An analysis of isostasy in the world's oceans, I, Hawaiian-Emperor seamount chain, *J. Geophys. Res.*, **83**, 5989-6004, 1978.
- Watts, A.B., and N.M. Ribe, On geoid heights and flexure of the lithosphere at seamounts, *J. Geophys. Res.*, **89**, 11,152-11,170, 1984.
- Watts, A.B., J.R. Cochran, and G. Selzer, Gravity anomalies and flexure of the lithosphere: A three-dimensional study of the Great Meteor Seamount, northeast Atlantic, *J. Geophys. Res.*, **80**, 1391-1399, 1975.
- Watts, A.B., J.H. Bodine, and N.M. Ribe, Observations of flexure and the geological evolution of the Pacific Ocean basin, *Nature*, **283**, 532-537, 1980.
- White, W.M., and R.A. Duncan, Geochemistry and geochronology of the Society Islands: New evidence for deep mantle recycling, in *Earth Processes: Reading the Isotopic Code*, *Geophys. Monogr. Ser.* vol 95, edited by A. Basu and S. Hart, pp. 183-206, AGU, Washington, D.C., 1996.
- Young, R.Y., and I.A. Hill, An estimate of the effective elastic thickness of the Cape Verde Rise, *J. Geophys. Res.*, **91**, 4854-4866, 1986.

---

V. Clouard and A. Bonneville, Laboratoire de Géosciences Marines et Télédétection, Université de la Polynésie Française, BP 6570 Faaa Aéroport, Tahiti, French Polynesia. (clouard@ufp.pf; bonneville@ufp.pf)

H.G. Barszczus, GBE - UMR 5569 - CNRS, and Université de Montpellier II, 34095 Montpellier Cedex 5, France. (e-mail: barszczus@dstu.univ-montp2.fr)

(Received January 29, 1998; revised October 8, 1999; accepted November 4, 1999.)